

1 **Predictability of tropical Pacific decadal variability is dominated by oceanic**
2 **Rossby waves**

3 **(Supplementary material)**

4
5 Xian Wu^{1*}, Stephen G. Yeager², Clara Deser², Antonietta Capotondi^{3,4}, Andrew T. Wittenberg⁵,
6 and Michael J. McPhaden⁶

7
8 *1 Atmospheric and Oceanic Sciences Program, Princeton University, Princeton, NJ*

9 *2 National Center for Atmospheric Research, Boulder, CO*

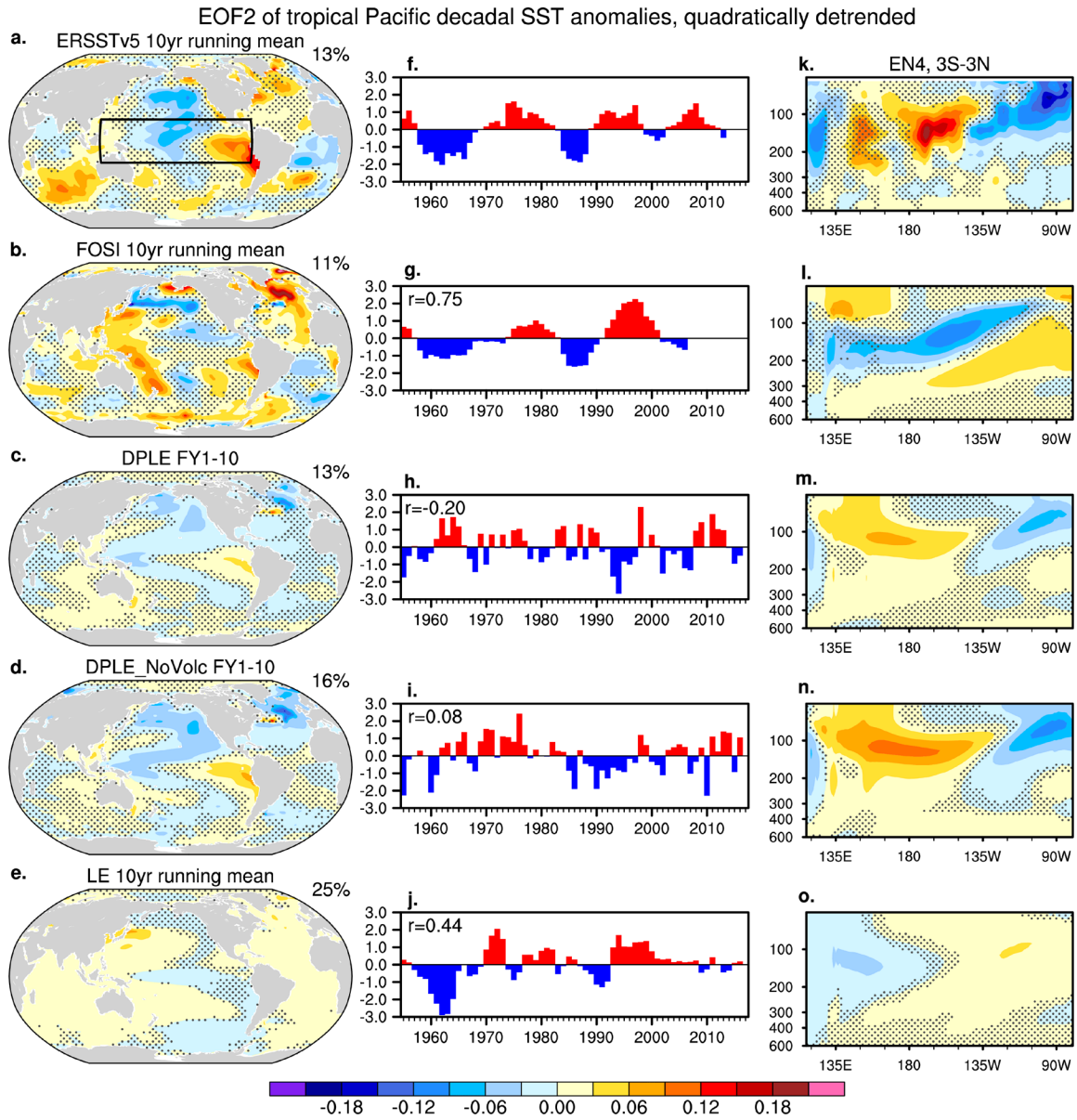
10 *3 Cooperative Institute for Research in Environmental Sciences, University of Colorado*
11 *Boulder, Boulder, CO*

12 *4 National Oceanic and Atmospheric Administration /Physical Sciences Laboratory, Boulder,*
13 *CO*

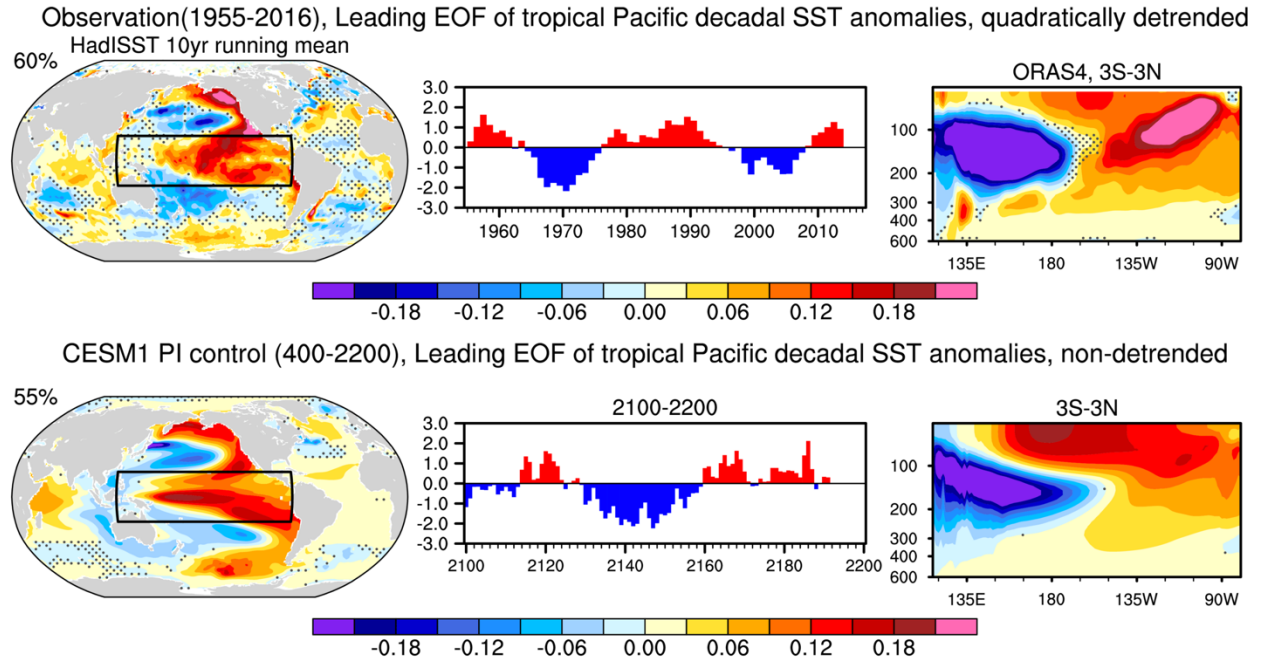
14 *5 National Oceanic and Atmospheric Administration/Geophysical Fluid Dynamics Laboratory,*
15 *Princeton, NJ*

16 *6 National Oceanic and Atmospheric Administration /Pacific Marine Environmental Laboratory,*
17 *Seattle, WA*

18
19
20
21
22
23
24
25
26 **Corresponding author: Xian Wu, xw2794@princeton.edu*

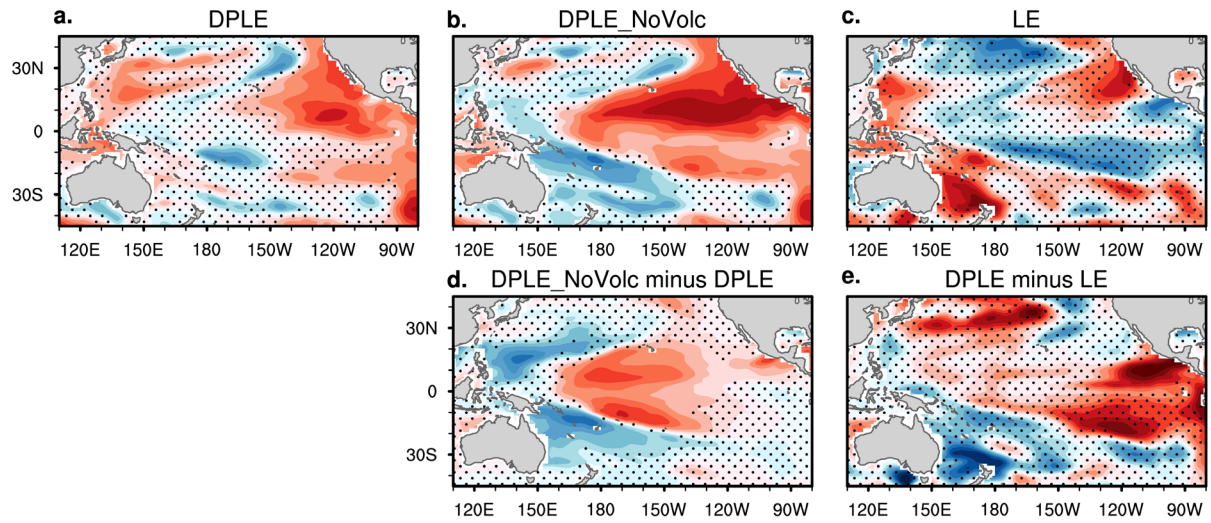


27
28 **Fig. S1** As in Fig. 1 but for the second leading EOF mode and PC2.

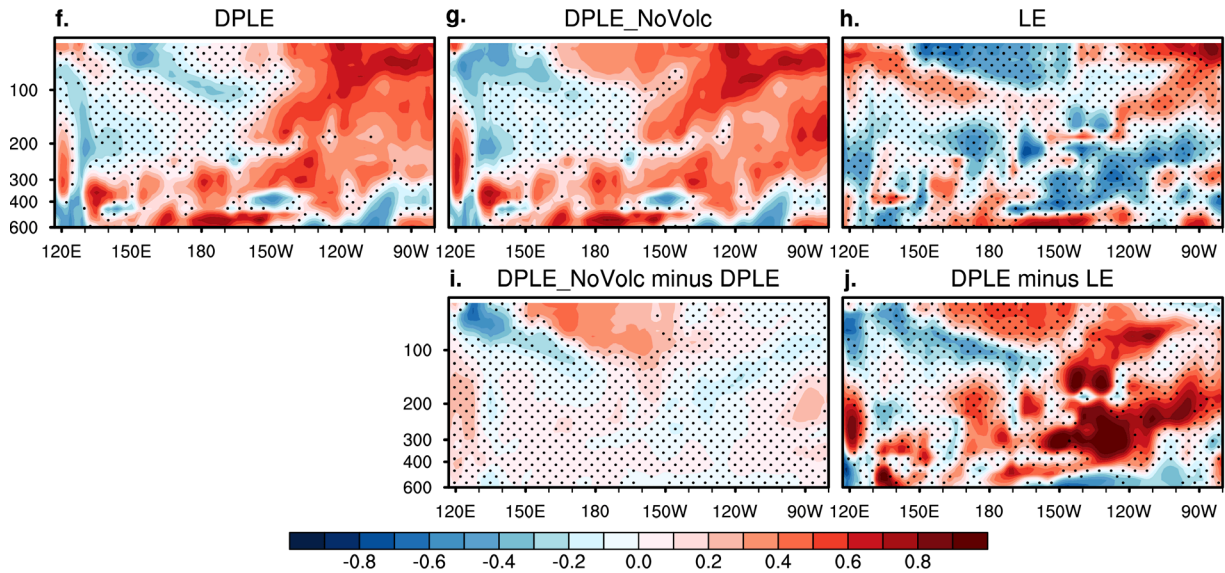


29
 30 **Fig. S2 TPDV simulation in the alternative observational datasets and the CESM1 free-**
 31 **running preindustrial simulation.** As in Fig. 1 in the main text, but for (top row) HadISST
 32 (1955–2022) and ORAS4 (1958–2019), and (bottom) 1801-yr control simulation of CESM1 under
 33 the preindustrial forcing condition. The timeseries of standardized PC1 are only shown for the last
 34 101 years (2100–2200). The year in the axis indicates the start year of any 10-year average window.
 35 The numbers in the top-left corner of panels in the first column denote the percentage of total
 36 variance explained by the leading EOF mode in each dataset.

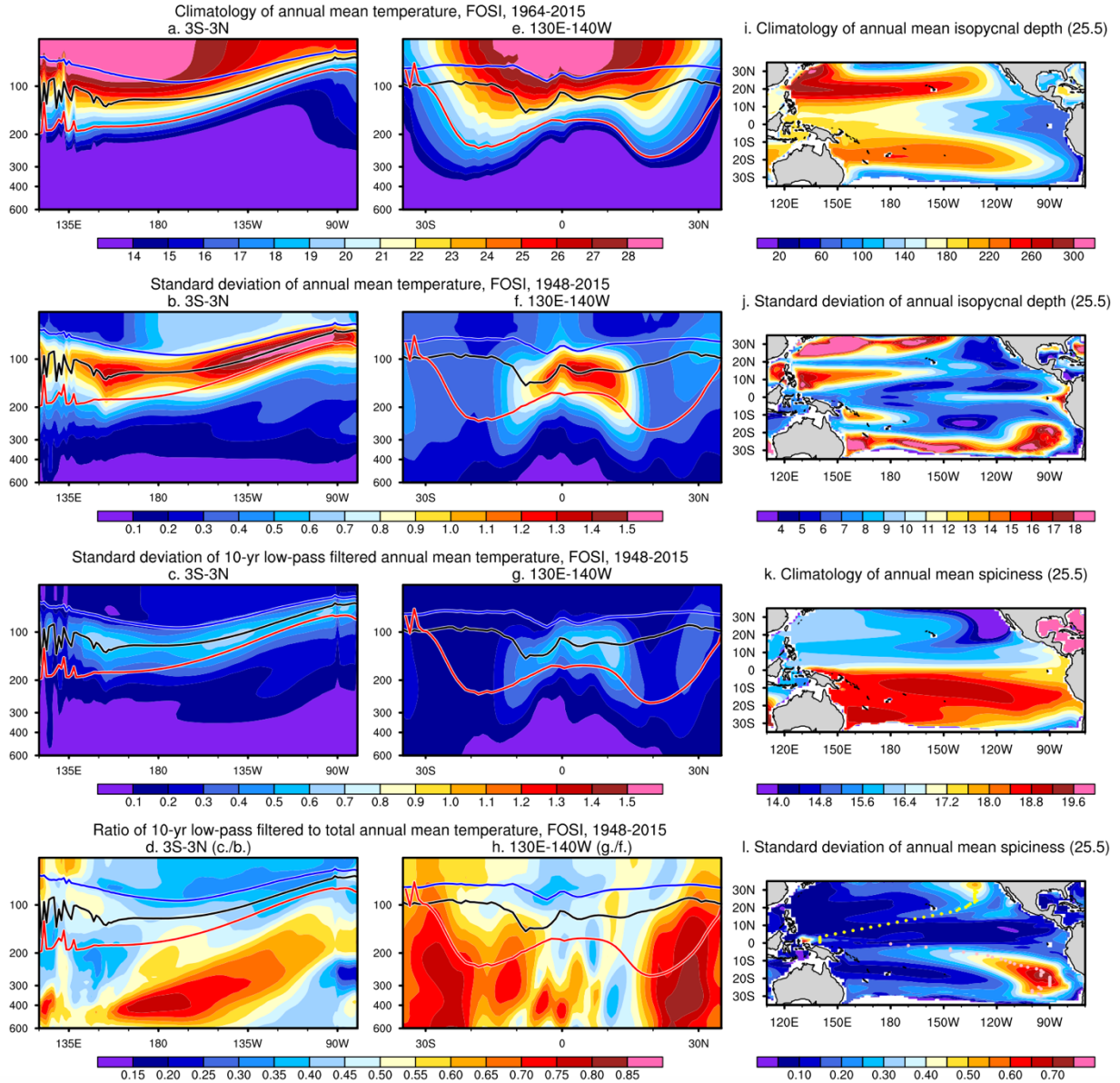
ACC of annual mean SST, FY1-10, quadratically detrended, verification data: ERSSTv5 1955-2022



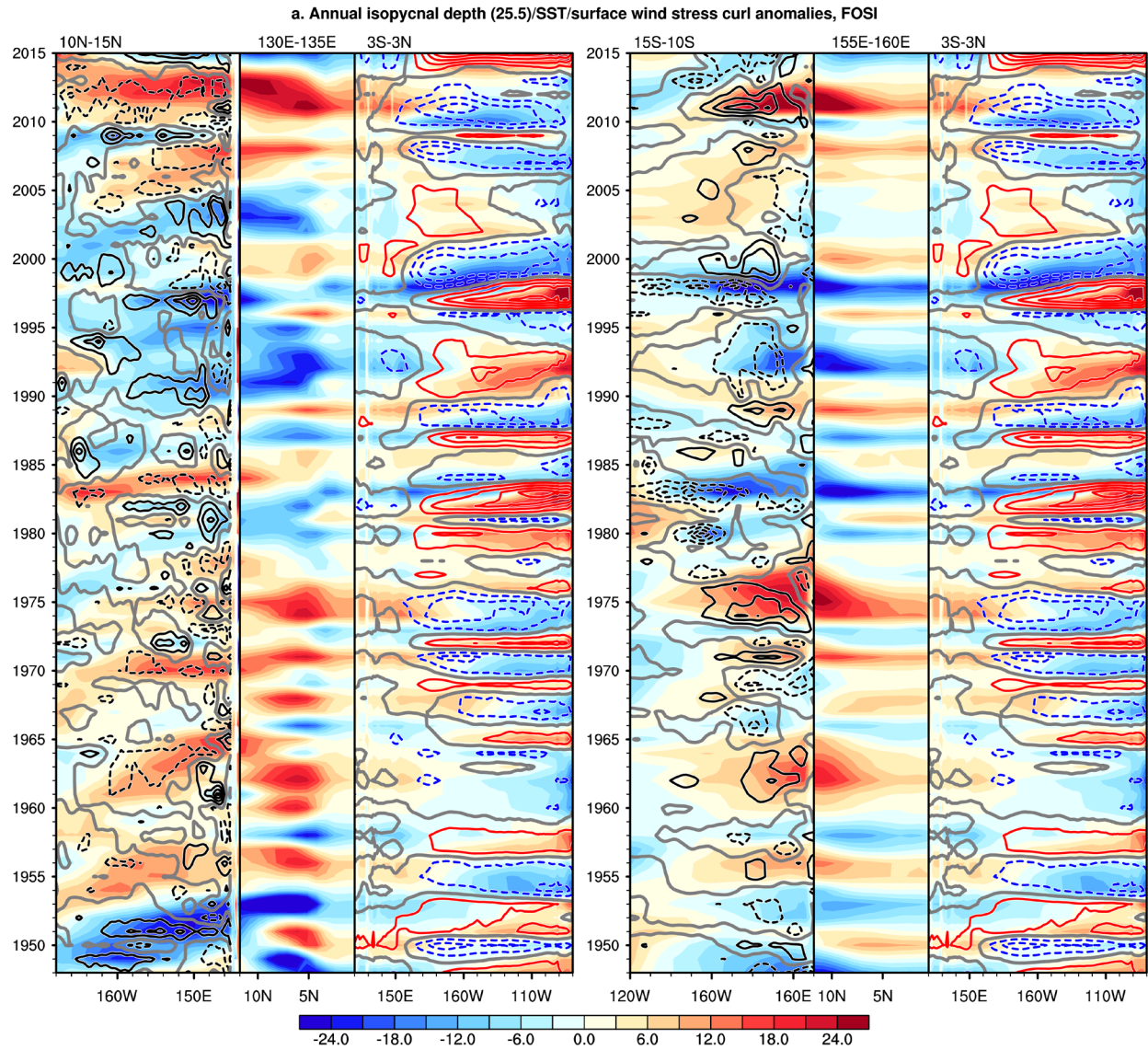
ACC of annual mean ocean temperature (3S-3N), FY1-10, quadratically detrended, verification data: EN4 1955-2022



37
38 **Fig. S3** As in Fig. 2 in the main text, but for skill evaluation relative to observations (SST in
39 ERSSTv5, and ocean temperature in EN4).

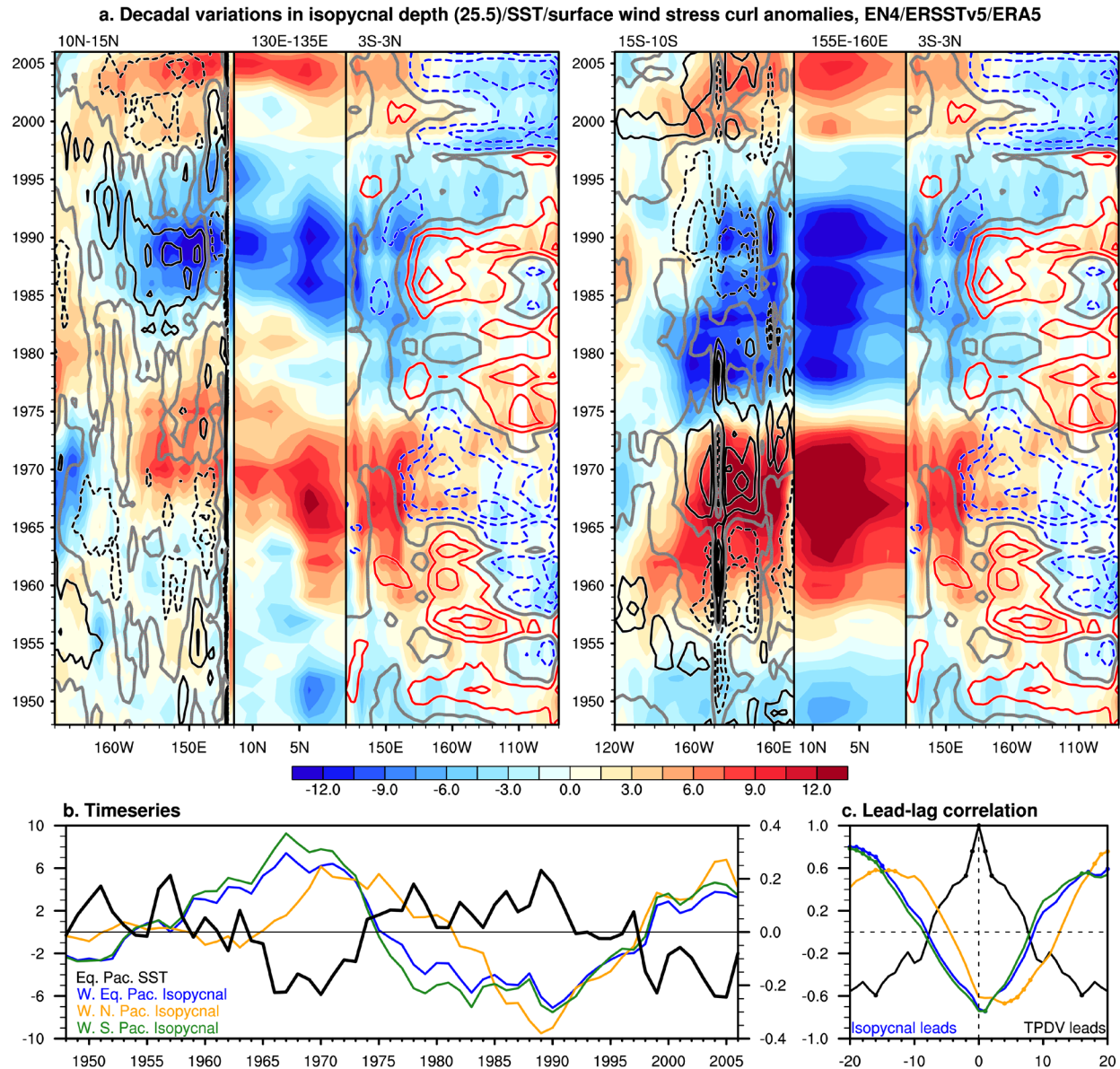


40
 41 **Fig. S4 Definition of different metrics capturing subsurface ocean temperature variability in**
 42 **FOSI.** (a) Climatology and (b) standard deviation of equatorial Pacific (3°S–3°N) subsurface
 43 ocean temperature, (c) standard deviation of 10-yr low-pass filtered component, and (d) standard
 44 deviation ratio of low-pass filtered component of total (non-detrended) annual mean temperature.
 45 (e-h) as in a–d but for the zonally averaged (130°E–140°W) subsurface ocean temperature. The
 46 curves in a–h denote the climatological mixed layer depth (blue curves), thermocline depth
 47 (defined as the depth of maximum vertical temperature gradient; black curves), and isopycnal
 48 depth where the potential density is equal to 25.5 kg m⁻³ ($\sigma_{\theta}=25.5$ kg m⁻³; red curves). (i)
 49 Climatology and (j) standard deviation of annual mean isopycnal depth ($\sigma_{\theta}=25.5$ kg m⁻³). (k)
 50 Climatology and (l) standard deviation of annual mean spiciness [°C; defined as temperature on
 51 the isopycnal depth ($\sigma_{\theta}=25.5$ kg m⁻³)]. The yellow and pink dots in l denote pathways where
 52 spiciness standard deviations are largest at each latitude.



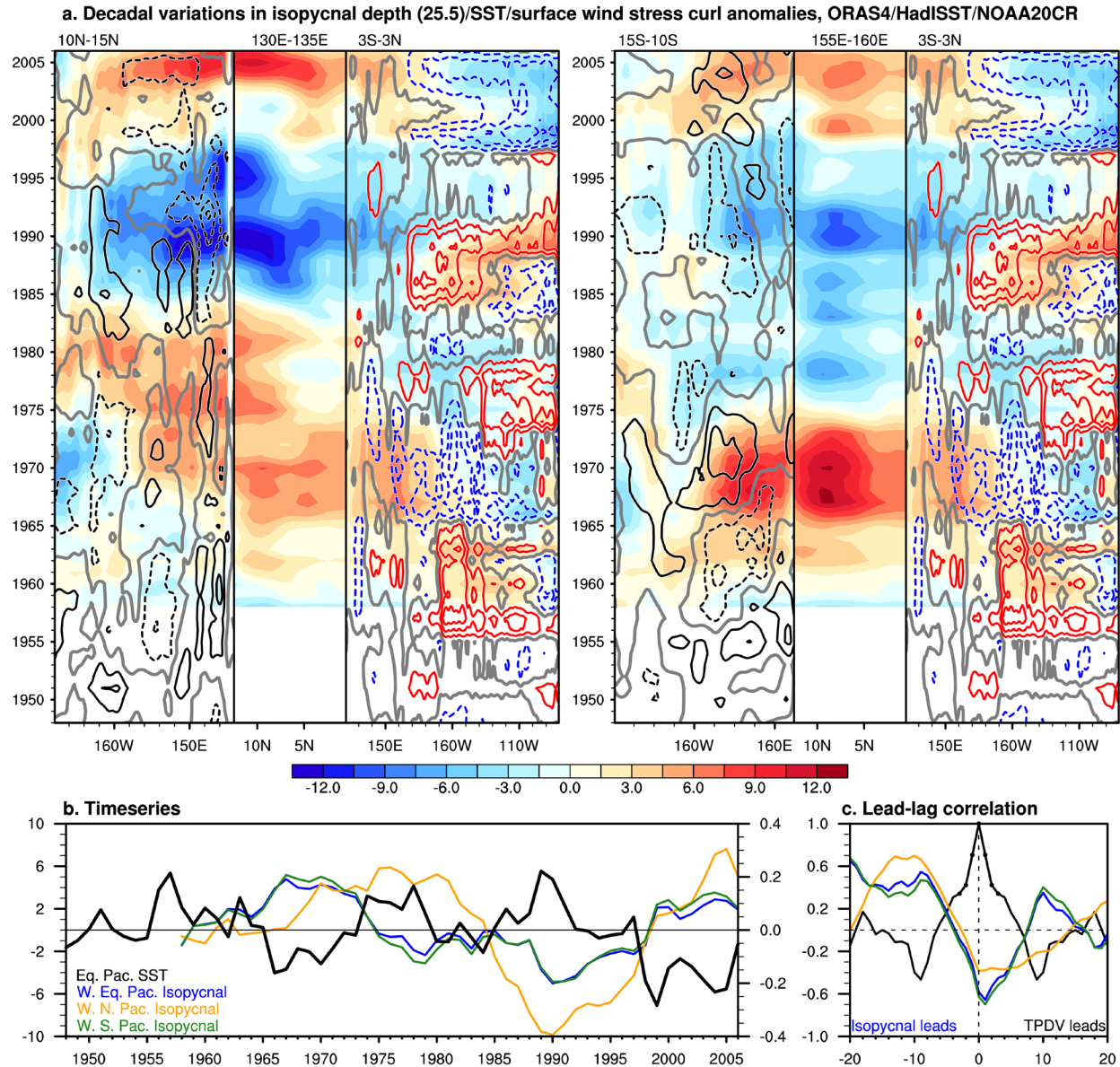
53
54

Fig. S5 As in Fig. 3a, but for non-filtered annual mean fields.



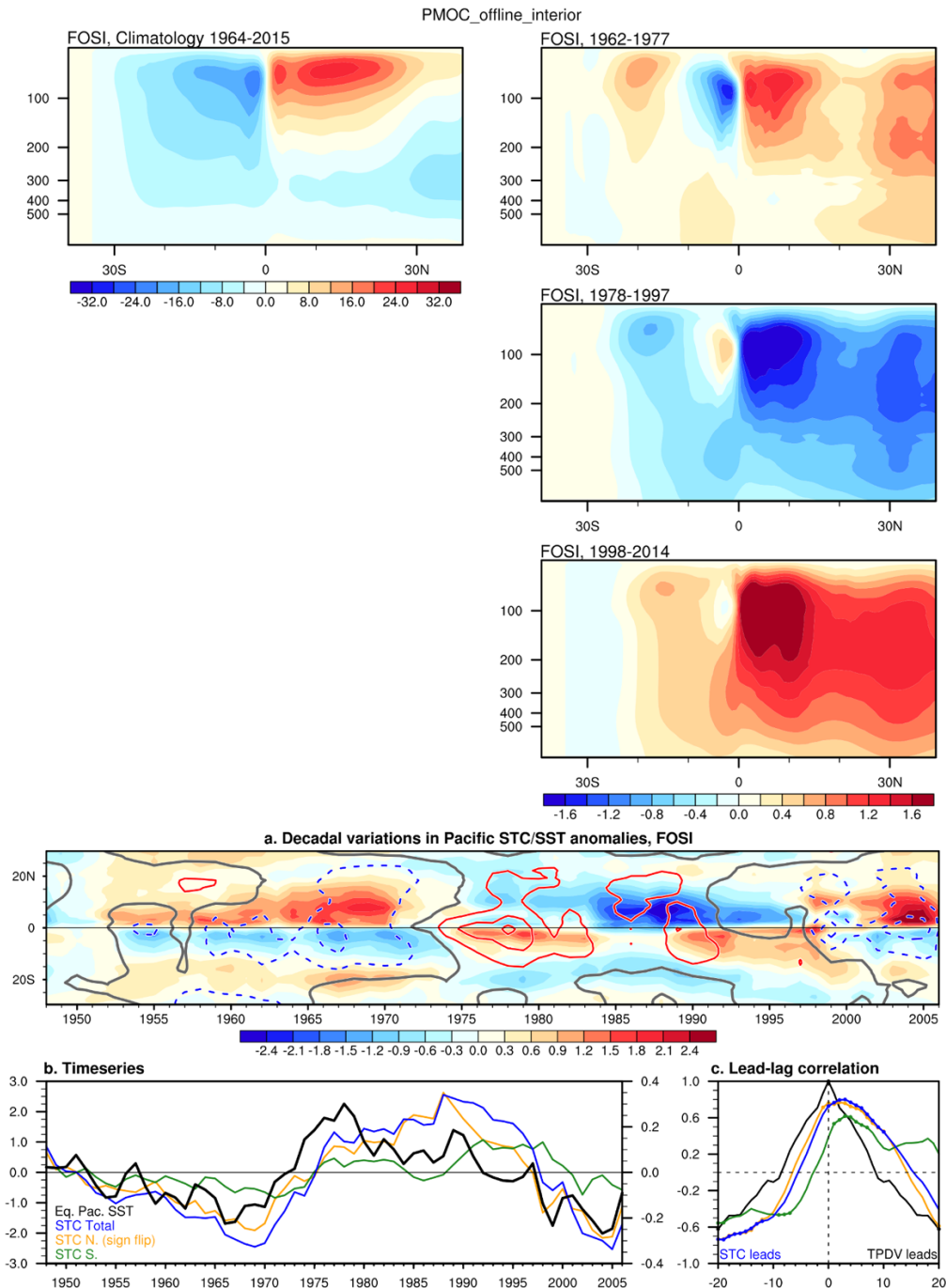
55
56
57

Fig. S6 As in Fig. 3, but using EN4 for isopycnal depth, ERSSTv5 for SST, and ERA5 for surface wind stress curl.



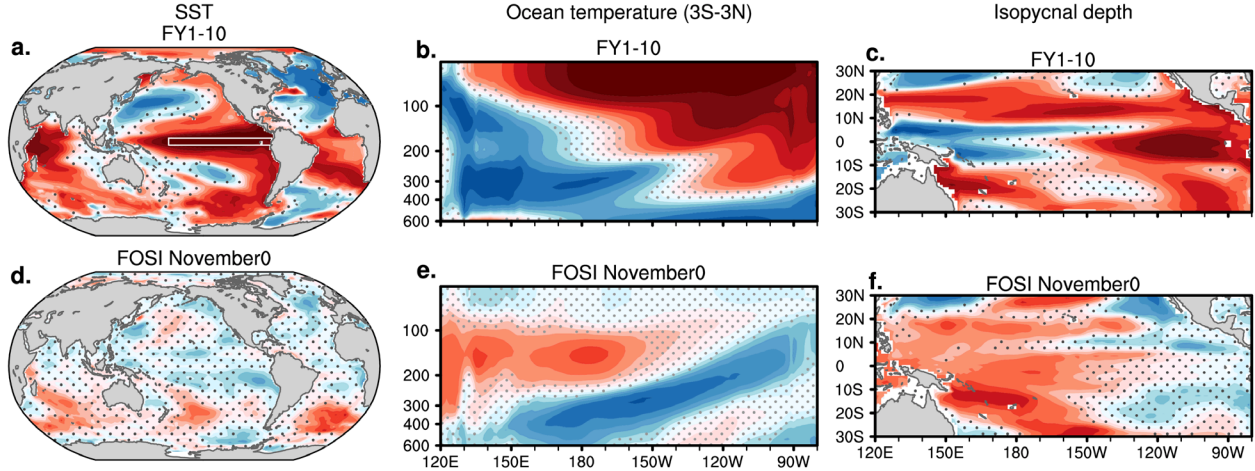
58
59
60

Fig. S7 As in Fig. 3, but using ORAS4 for isopycnal depth, HadISST for SST, and NOAA20CRv3 for surface wind stress curl.

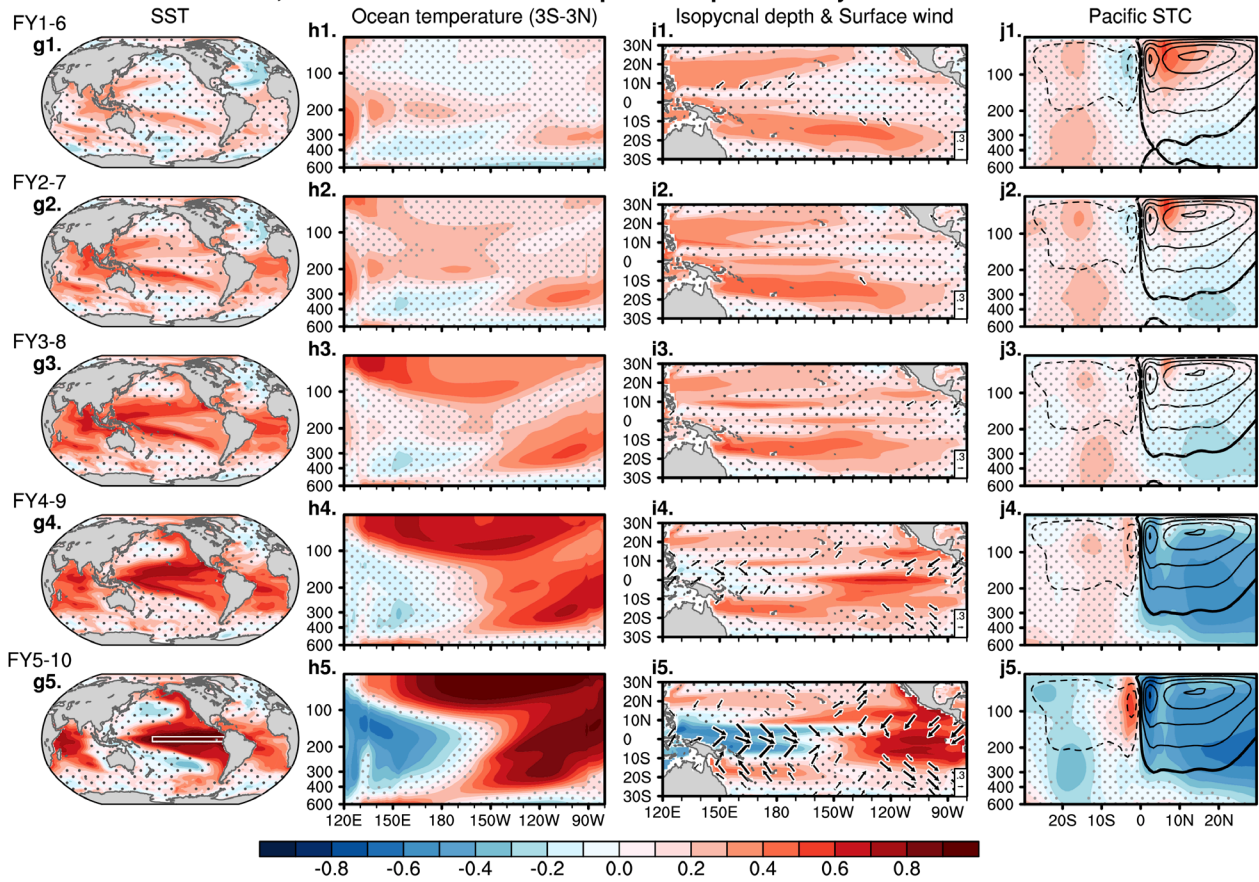


61
 62 **Fig. S8 STC climatology and anomalies associated with TPDV.** (top left) Climatology of
 63 zonally integrated interior (which excludes the western boundary currents) ocean overturning
 64 streamfunction (Sv) as a function of depth (m) and latitude. The zonal integration is taken from
 65 the Pacific eastern boundary to 145°E for the Northern Hemisphere and from the eastern boundary
 66 to 160°E for the Southern Hemisphere. Postive (negative) values of overturning streamfunction
 67 indicate clockwise (anti-clockwise) orbit direction of the transport. (right) Anomalies during the
 68 negative TPDV phases (1962–1977; 1998–2014) and positive TPDV phase (1978–1997). (a–c) As
 69 in Fig. 4a–c, but based on the total Pacific zonally integrated transport that includes the western
 70 boundary currents.

DPLE, Correlations with FY1-10 Eq. Pacific quadratically detrended SST

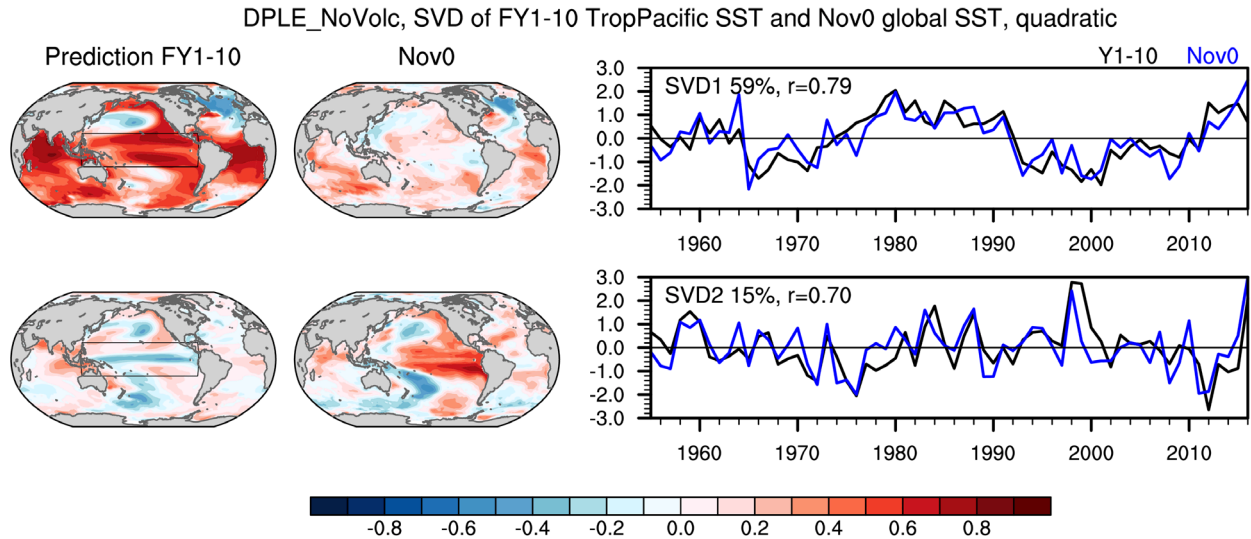


DPLE, Correlations with FY5-10 Eq. Pacific quadratically detrended SST



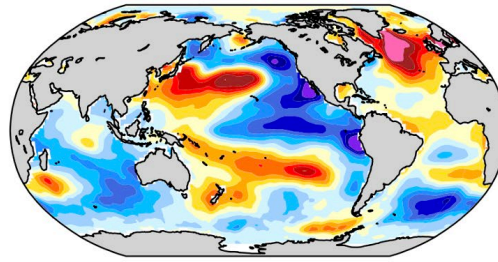
71
72
73

Fig. S9 As in Fig. 5, but for DPLE.

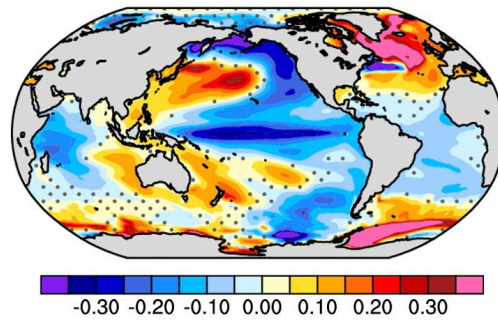


74
75 **Fig. S10** Pattern and timeseries associated with the (top row) first and (bottom row) second SVD
76 modes of the covariance of predicted tropical Pacific (20°S–20°N, 120°E–120°W) SST anomalies
77 in FY1–10 during 1955–2016, and global initial SST anomalies in Nov0 during 1954–2015. SVD1
78 explains 59% of the total squared covariance, while SVD2 explains 15%. The expansion
79 coefficients are correlated at a coefficient of 0.79 and 0.70 for SVD1 and SVD2, respectively. (left
80 column) Regression maps of predicted SST at FY1–10 on the standardized Nov0 SST expansion
81 coefficient (blue curve). (middle column) Regression maps of initial SST at Nov0 on the
82 standardized FY1–10 SST expansion coefficient. (right column) Standardized time series of FY1–
83 10 SST (black) and Nov0 SST (blue) expansion coefficients.
84

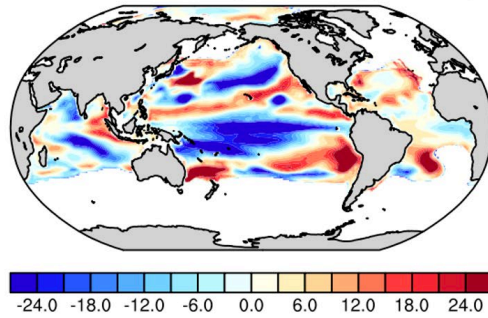
1999-2008, SST anomalies
a. ERSSTv5



b. CESM1 DPLE NoVolc



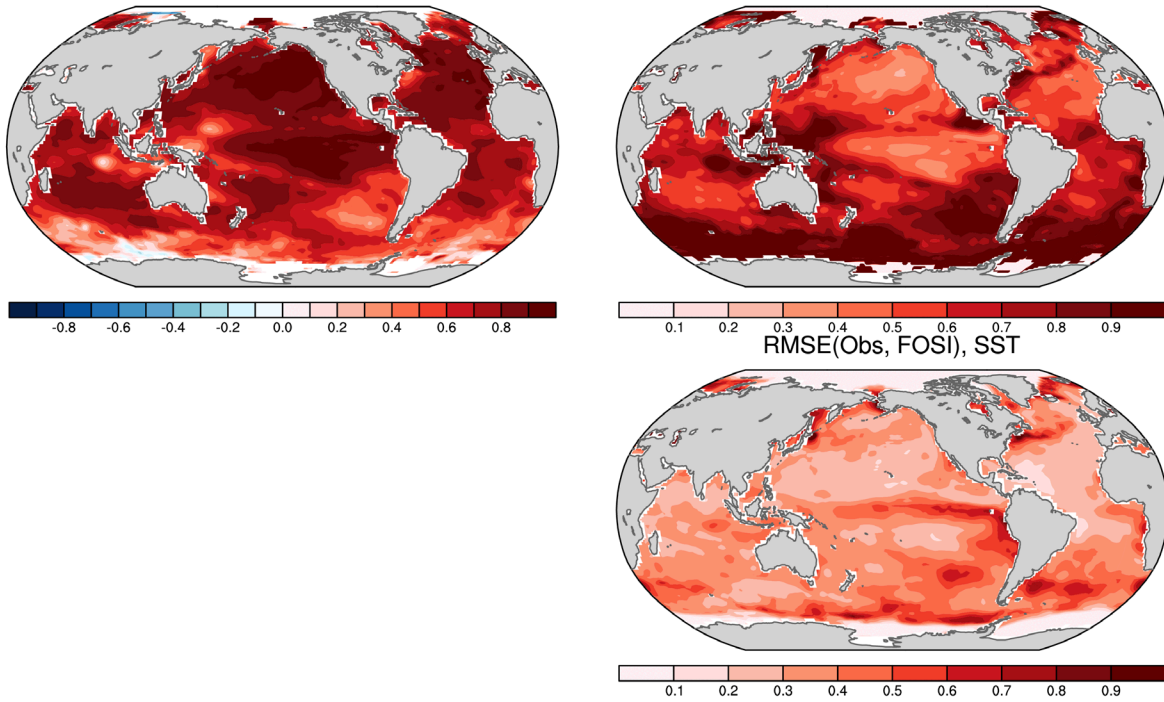
c. FOSI, Nov monthly mean isopycnal depth



85
86 **Fig. S11** Quadratically detrended SST anomalies during 1999–2008 in (a) ERSSTv5 and (b) the
87 10-member ensemble-mean forecast initialized in November 1998 in DPLE_NoVolc using
88 traditional drift correction method (see Methods). (c) Isopycnal depth anomalies (\bar{m} ; $\sigma_{\theta} = 25.5 \text{ kg}$
89 m^{-3}) on November 1, 1998, in FOSI.

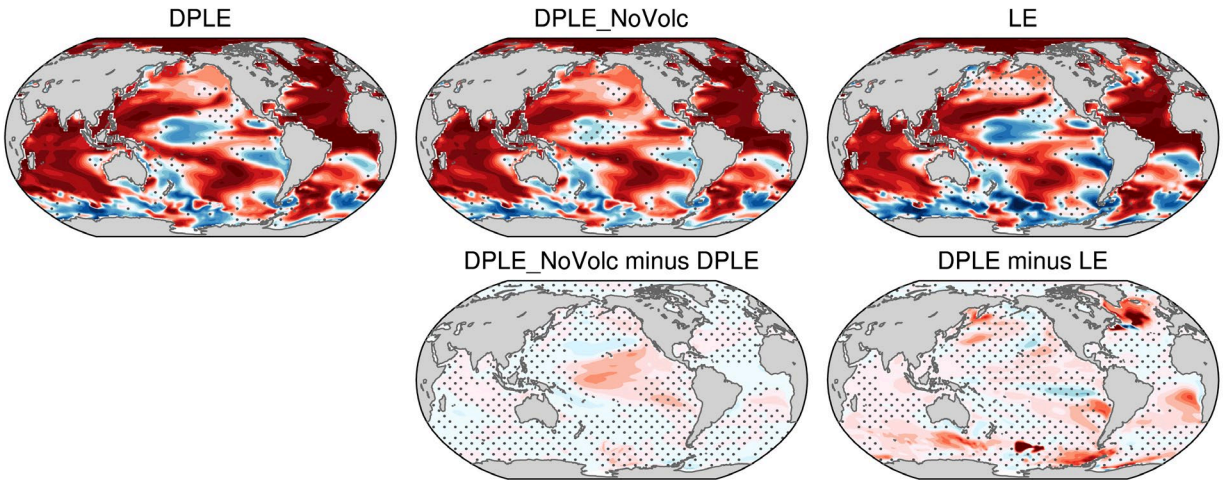
90
91

Evaluation of FOSI initial condition anomalies in November, 1954-2015, nondetrend
Corr(Obs, FOSI), SST
RMSE(Obs, FOSI)/RMS(Obs), SST

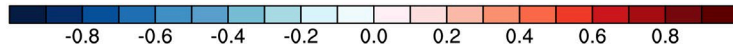
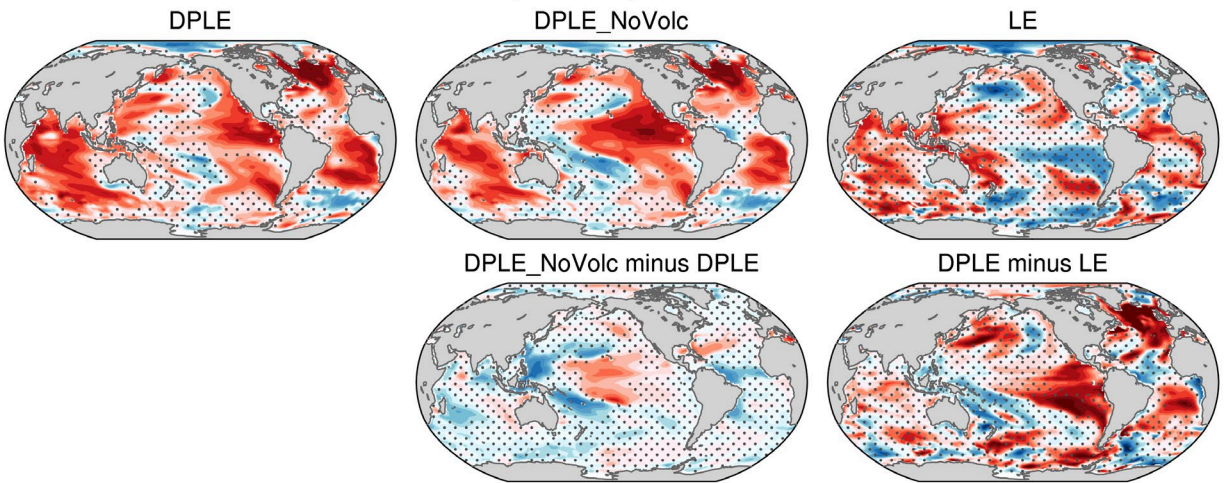


92
93 **Fig. S12 Evaluation of SST initial conditions in FOSI** (top left) Correlation, (top right)
94 standardized Root Mean Square Error (RMSE), and (bottom right) RMSE maps of SST in
95 November in FOSI compared to ERSSTv5 during 1954-2015.

ACC of annual mean SST, FY1-10, non detrended, verification data: FOSI 1955-2015

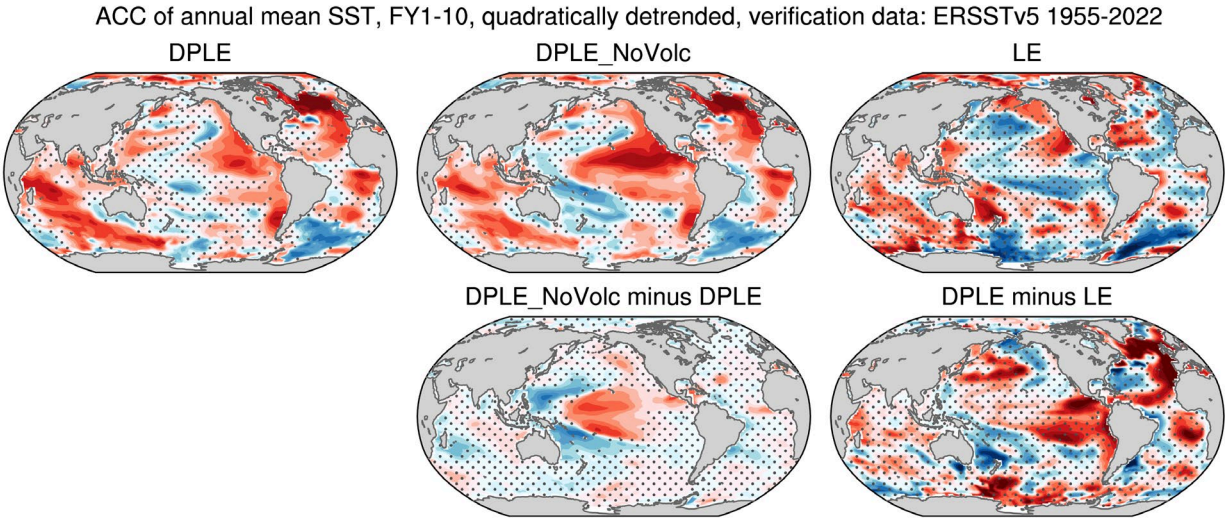
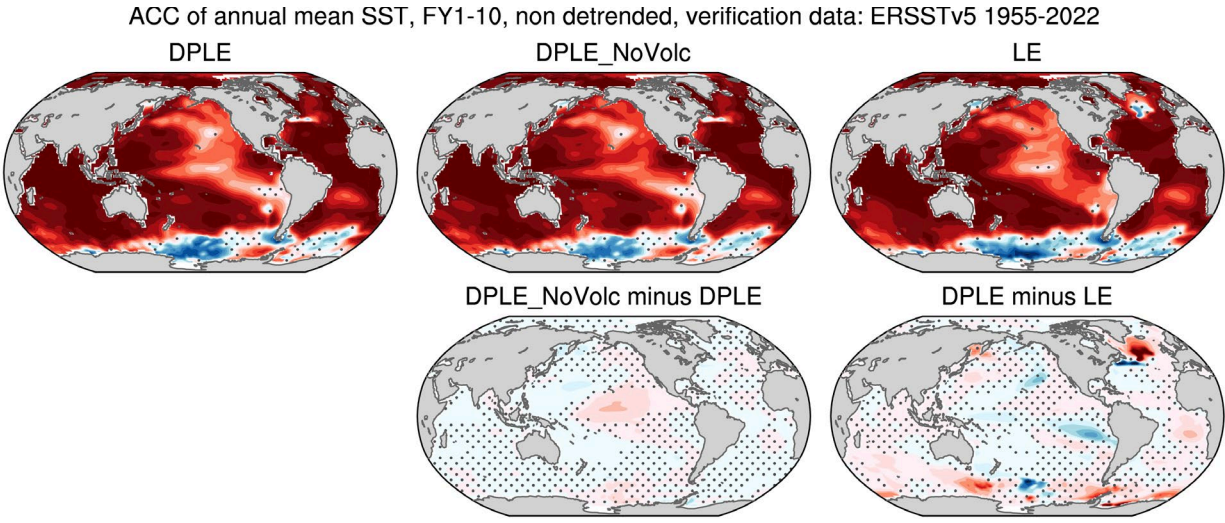


ACC of annual mean SST, FY1-10, quadratically detrended, verification data: FOSI 1955-2015



96
97
98

Fig. S13 As in Fig. 2a–e in the main text, but for skill evaluation for the global SST relative to FOSI.



99
100
101

Fig. S14 As in Fig. 2a–e in the main text, but for skill evaluation for the global SST relative to ERSSTv5.